Solar Energy Materials & Solar Cells 115 (2013) 145–150

Contents lists available at SciVerse ScienceDirect

Solar Energy Materials & Solar Cells

journal homepage: www.elsevier.com/locate/solmat

# Colored solar selective absorbing coatings with metal Ti and dielectric AlN multilayer structure

Yangwei Wu, Weifeng Zheng, Limei Lin, Yan Qu, Fachun Lai *

*College of Physics and Energy, Fujian Normal University, Fuzhou 350108, PR China*

ARTICLE INFO

*Article history:*
Received 18 October 2012
Received in revised form
25 March 2013
Accepted 29 March 2013

*Keywords:*
Colored solar collectors
Architectural integration
Chromaticity
Multilayer structure
Optical constants

ABSTRACT

The colored solar–thermal collectors have the advantages of architectural integration and color appearance. The solar selective absorbing coatings with a metal–dielectric multilayer structure can show different colors by changing the layer number and thickness. In this work, five colored coatings with a metal titanium (Ti) and dielectric aluminum nitride (AlN) multilayer structure were designed by the optical multilayer software and fabricated by magnetron sputtering. The color of the five coatings is black, purple, yellowish green, red, and yellowish orange. The energy performance, chromaticity, and brightness of the coatings were studied and compared. The results show that the solar absorbance of these coatings is between 0.82 and 0.94, the thermal emittance is between 0.05 and 0.27, and the brightness is in the range of 0.65–8.89%. These colored coatings can be produced by a commercial production process, and is suitable for the application of building integration.



## 1. Introduction

Solar–thermal collectors with high absorbance and low thermal emittance have been used for converting solar energy into thermal energy [1,2]. The collector absorbing surface is usually black in order to maximize the absorption of the solar spectrum. However, the black color of the collectors on building roofs and facades limits the architectural integration into buildings [3–6]. Moreover, a survey presents that 85% of architects would prefer colored solar collectors other than black ones [4,7,8]. Therefore, it is important to fabricate colored collectors with high solar–thermal conversion efficiency.

Previously, several methods have been proposed to fabricate colored collectors, such as spectrally selective colored paint [5,6], colored glazed collectors based on thin film interference filters [7,9–12], and colored absorbing coatings [8,13]. Amongst these, the colored absorbing coatings have the advantages of a good thermal stability and a low cost in production.

Both wet chemical methods [14,15] and physical vapor deposition [2,8,16] have been used to prepare solar selective coatings. Based on physical vapor deposition, the magnetron sputtering technique is widely used to produce the absorbing coatings with a metal–dielectric composited structure [2], owing to the good chemical and thermal stabilities of its products. Accordingly, the solar selective coatings with a metal–dielectric multilayer structure were also prepared by the magnetron sputtering method [17–19], which has the advantages of good reproducibility, spectral stability in the deposition process, and satisfying the commercial requirements of a mass production process [18,19]. However, a systematic research about the colored absorbing coating with a metal–dielectric multilayer structure still remains to be reported.

In this work, the colored solar selective absorbing coatings with a metal–dielectric multilayer structure were designed by the optical multilayer design software and fabricated by the magnetron sputtering technique. The optical constants of metal titanium (Ti) and dielectric aluminum nitride (AlN) films with different thicknesses were retrieved from the reflectance or transmittance values. Energy performance, chromaticity, and brightness of the colored coatings were studied.

## 2. Experimental details

In order to obtain the optical constants of AlN and Ti single layer films, dielectric AlN films with different thicknesses were deposited on quartz substrates using a metal Al target (99.99% in purity) by the reactive dc magnetron sputtering. Accordingly, metal Ti films with different thicknesses were deposited using a metal Ti target (99.99% in purity) by the non-reactive dc magnetron sputtering. The substrates, 0.5 mm thick, 2.5 cm × 2.5 cm, were cleaned in acetone and ethanol several times before deposition. The distance between the substrate and target was 13 cm. The base pressure of the vacuum chamber was $4.0 \times 10^{-4}$ Pa and the sputtering power was 100 W. The thickness of the film was controlled by the sputtering

* Corresponding author. Tel.: +86 591 22868137; fax: +86 591 22868132.
*E-mail address:* laifc@fjnu.edu.cn (F. Lai).

0927-0248/$ - see front matter © 2013 Elsevier B.V. All rights reserved.
http://dx.doi.org/10.1016/j.solmat.2013.03.041

time according to the deposition rate. Before the deposition of Ti–AlN multilayer coatings, a Cu layer with thickness about 120 nm was deposited on quartz substrate using a metal Cu target (99.99% in purity) by the dc magnetron sputtering. The deposition parameters of Cu, Ti, and AlN layers are summarized in Table 1. Five colored solar absorbing coatings with a Ti–AlN multilayer structure were prepared, and the Ti and AlN layers were deposited at the above conditions. The color of the coatings is black, purple, yellowish green, red, and yellowish orange.

The normal incidence transmittance ($T$) and total reflectance ($R$) of the samples were recorded in the wavelength range of 300–2500 nm with a spectral resolution of 1.0 nm by a double-beam spectrophotometer (Perkin-Elmer Lambda 950). It was equipped with an integrating sphere for measurements of total $R$. Infrared spectra were acquired with a Perkin-Elmer Spectrum One Fourier transform infrared (FTIR) spectrophotometer in the range of 2.5–25 μm (4000–400 $cm^{-1}$). FTIR spectra were measured with a 10° specular reflectance accessory and a gold substrate alignment mirror at room temperature and the spectral resolution is about 0.9 $cm^{-1}$.

## 3. Optical constant deduction

Many methods for the determination of optical constants have been reported [20–28]. Generally, the optical constants of a film were retrieved by simulating the experimental ellipsometric spectra [21–24], transmittance or reflectance [25–28] based on the optical dielectric models. We have determined the optical constants and thickness of an $In_2O_3$:Sn film from transmittance data based on the Forouhi–Bloomer model combined with the modified Drude model in our previous research results [26]. In this research, Ti film is a metal film and AlN is a dielectric film. Therefore, the optical constants of AlN film were calculated by the Forouhi–Bloomer model combined with the modified Drude model [26,27]. For the Ti film, the Drude–Lorentz model was used to determine the optical constants, which combines the Drude model with the Lorentz oscillator model. The dielectric function of the Drude–Lorentz model can be expressed as [24,28]

$$\varepsilon_{DL}(\omega)=\varepsilon_b-\frac{\omega_D^2}{\omega^2-i\gamma_D\omega}+\sum_j\frac{C_j}{\omega_j^2-\omega^2-i\gamma_j\omega} \tag{1}$$

where $\omega$ is the frequency, and the constant ($\varepsilon_b$) depends on the contribution to the dielectric constants beyond the simulated spectral range. The second part in Eq. (1) stands for the contribution of the Drude model, where $\omega_D$ in Eq. (1) is the plasma frequency and $\gamma_D$ is the Drude damping constant. The last part is the Lorentz model, where $\omega_j$ and $\gamma_j$ are the frequency and damping terms of a particular resonance line, and $C_j$ is the amplitude of this resonance line.

Based on the optical dielectric models, two computer programs were written in FORTRAN for calculating the optical constants and thicknesses of the metal film and dielectric film using a nonlinear least squares arithmetic. As a result, the optical constants and thickness of AlN film were calculated from the measured transmittance data, and those of Ti film were calculated from the measured reflectance and transmittance data.

**Table 1**
Sputtering parameters for the depositions of Cu, Ti, and AlN layers.

| Layer | Ar flow rate (sccm) | $N_2$ flow rate (sccm) | Thickness (nm) | Sputtering pressure (Pa) |
|---|---|---|---|---|
| Cu | 42.5 | – | 120 | 0.7 |
| Ti | 42.5 | – | 18, 24, 31 | 0.7 |
| AlN | 40 | 8 | 63, 85, 265 | 1.6 |

## 4. Energy performance, chromaticity, and brightness

### 4.1. Energy performance

The energy performance of a solar selective absorbing coating is expressed by two basic parameters of solar absorbance ($\alpha$) and thermal emittance ($\varepsilon$), when transmittance is zero, which can be calculated by [14]

$$\alpha=\frac{\int_{0.3}^{2.5}(1-R(\lambda))I_s(\lambda)d\lambda}{\int_{0.3}^{2.5}I_s(\lambda)d\lambda} \tag{2}$$

$$\varepsilon=\frac{\int_{2.5}^{25}(1-R(\lambda))I_b(\lambda,\ t)d\lambda}{\int_{2.5}^{25}I_b(\lambda,\ t)d\lambda} \tag{3}$$

where $\lambda$ is the wavelength (integral borders in μm), $R(\lambda)$ is the reflectance at $\lambda$, $I_s(\lambda)$ is the solar spectral radiation at AM=1.5, and $I_b(\lambda,t)$ is the black body spectral radiation, $t$=80 °C is used for the normal temperature solar–thermal application. Note that the upper integral borders of 25 μm ($\alpha$) and 2.5 μm ($\varepsilon$) are due to limitations in the spectrometers, and hence do not cover the whole solar radiation spectrum and infrared spectrum, where ideally the upper borders should have been 3 μm and 50 μm (or even 100 μm), respectively.

### 4.2. Chromaticity

According to the description of the $XYZ$ color system by the International Commission on Illumination (CIE) in 1931, the tristimulus values $X$, $Y$ and $Z$ are computed from the measured or simulated spectral power distribution data $P(\lambda)$ by [7,8,27]

$$X=\int_{380}^{780}P(\lambda)\bar{x}(\lambda)d\lambda \tag{4}$$

$$Y=\int_{380}^{780}P(\lambda)\bar{y}(\lambda)d\lambda \tag{5}$$

$$Z=\int_{380}^{780}P(\lambda)\bar{z}(\lambda)d\lambda \tag{6}$$

where $\lambda$ is the wavelength (integral borders in nm). $\bar{x}(\lambda)$, $\bar{y}(\lambda)$, and $\bar{z}(\lambda)$ are the CIE-1931 standard spectrum tristimulus values. In this work, $P(\lambda)=D_{65}(\lambda)R(\lambda)$, where $D_{65}$ is a standard illuminant and represents typical daylight. Then the color coordinates $x$, $y$, and $z$ are calculated by

$$x=\frac{X}{X+Y+Z} \tag{7}$$

$$y=\frac{Y}{X+Y+Z} \tag{8}$$

$$z=1-(x+y) \tag{9}$$

### 4.3. Brightness

When a surface appears to the human eye under certain illumination conditions, the brightness is determined by its visible reflectance $R_{VIS}$, and can be written as [7,10,27]

$$R_{VIS}=\frac{\int_{0.4}^{0.7}R(\lambda)I_{ILL}(\lambda)V(\lambda)d\lambda}{\int_{0.4}^{0.7}I_{ILL}(\lambda)V(\lambda)d\lambda} \tag{10}$$

where $I_{ILL}(\lambda)$ is the illuminant at $\lambda$ (integral borders given in μm), and $V(\lambda)$ is the photopic luminous efficiency function.

## 5. Results and discussion

### 5.1. Optical constants of AlN and Ti films

The optical constants of a dielectric film may change with film thickness [29,30]. So AlN films with thicknesses of 63 nm, 85 nm, and 265 nm were prepared and their transmittances are shown in Fig. 1. Transmittance is higher than 85% and the highest transmittance (about 93%) is close to that of bare substrate because AlN is a transparent material. The optical constants and thicknesses were calculated from the data in Fig. 1 and the calculated transmittance (dashed line) is in good agreement with the measured datum. Fig. 2 presents refractive index ($n$) and extinction coefficient ($k$) of AlN films. $n$ is between 1.6 and 1.7, and $k$ is lower than 0.01. Moreover, both $n$ and $k$ increase with increasing thickness, which is due to the densification as the thickness increases.

According to Savaloni and Shayegan's research report [23], the optical constants of Ti film deposited by magnetron sputtering change with film thickness. So Ti films with thicknesses of 18 nm, 24 nm, and 31 nm were prepared, whose transmittance and reflectance are presented in Fig. 3. Transmittance decreases and reflectance increases with increasing thickness owing to the metallicity of Ti. Based on the transmittance and reflectance data in Fig. 3, the optical constants of Ti films were calculated by Eq. (1) and the results are indicated in Fig. 4. The calculated reflectance and transmittance (dashed lines) of 24 nm thick Ti film are also shown in Fig. 3 and are consistent and in good agreement with the measured spectra. As indicated in Fig. 4, $n$ of Ti films is between 1.9 and 4.1, and $k$ is between 0.5 and 1.8. Both $n$ and $k$ increase with increasing film thickness.

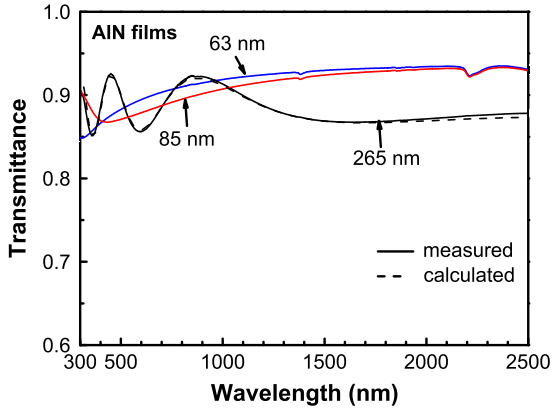


**Fig. 1.** Measured transmittance of AlN films with different thicknesses, the dashed line is the calculated transmittance of the 265 nm thick film.

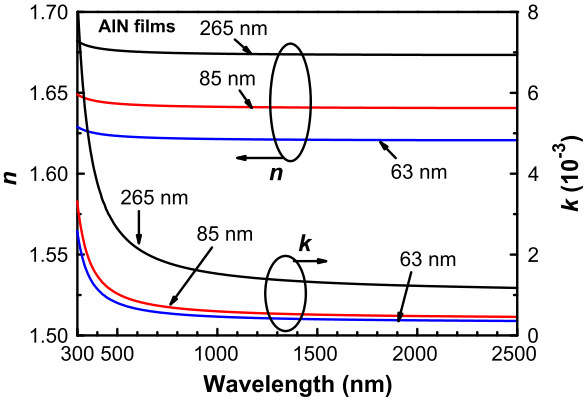


**Fig. 2.** Refractive indices ($n$) and extinction coefficients ($k$) of AlN films with different thicknesses.

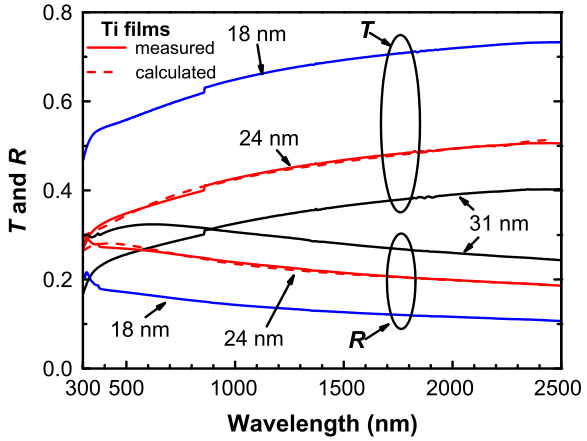


**Fig. 3.** Measured transmittance ($T$) and reflectance ($R$) of the Ti films with different thicknesses, the dashed lines are the calculated transmittance and reflectance of the 24 nm thick film.

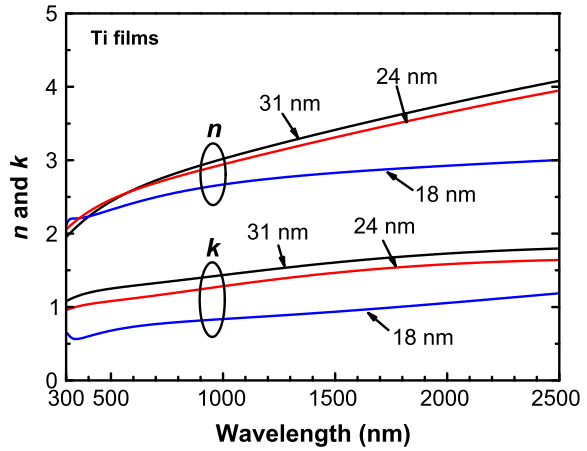


**Fig. 4.** Refractive indices ($n$) and extinction coefficients ($k$) of Ti films with different thicknesses.

### 5.2. Colored absorbing coatings

Based on the optical constants of Ti and AlN films in Figs. 2 and 4, five solar selective absorbing coatings were designed by the optical multilayer design software [27,31] at a wavelength of 300–2500 nm and fabricated by the dc magnetron sputtering. In the design process, layer number and thickness were optimized so that the sample has a color in the visible spectral region and a high solar absorbance. The colors of these samples are black, purple, yellowish green, red, and yellowish orange.

The maximum difference between the designed and measured reflectance of these samples at a given wavelength is about 5% when $\lambda < 1200$ nm, and is about 12% when $\lambda > 1200$ nm. As the examples, the designed and measured reflectance spectra of the purple and yellowish orange samples are shown in Fig. 5. For the purple sample, the measured reflectance is in good agreement with the designed reflectance at $\lambda < 590$ nm and $\lambda > 1150$ nm. The maximum difference between the designed reflectance and measured reflectance is about 4% at $\lambda = 920$ nm. As to the yellowish orange sample, the measured reflectance is consistent with designed reflectance at $\lambda$ between 450 nm and 1020 nm. The difference between the designed reflectance and measured reflectance has the maximum (5%) at $\lambda = 350$ nm. The results indicate that the solar absorbing coating can be produced according to the design by magnetron sputtering.

Fig. 6 shows the reflectance of the black sample. As presented in the left inset in Fig. 6, this coating is a Ti–AlN–Ti–AlN four layers

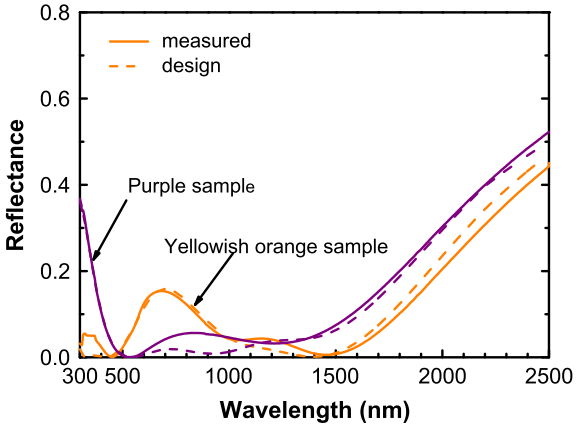


**Fig. 5.** Designed and measured reflectance spectra of the purple and yellowish orange samples. (For interpretation of the references to color in this figure legend, the reader is referred to the web version of this article.)

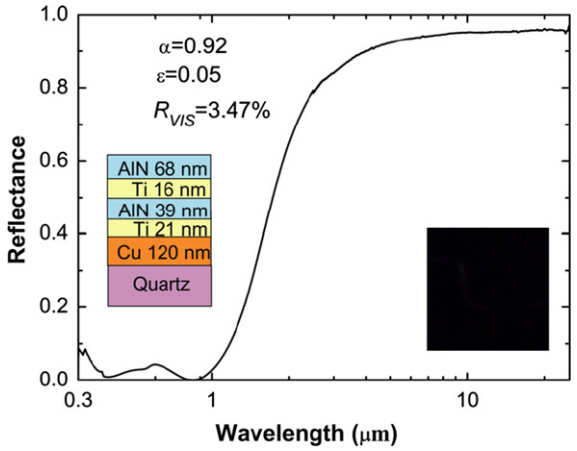


**Fig. 6.** Reflectance of the black sample. Left inset illustrates each material layer and thickness, and right inset is the sample color taken from photograph.

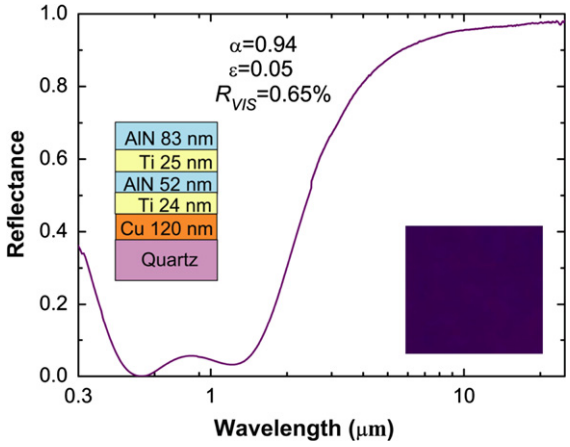


**Fig. 7.** Reflectance of the purple sample. (For interpretation of the references to color in this figure legend, the reader is referred to the web version of this article.)

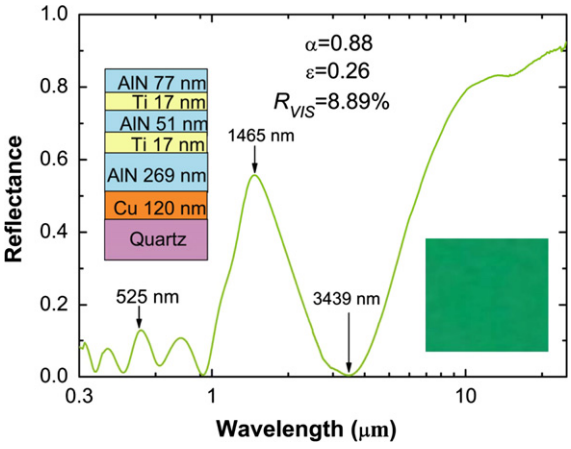


**Fig. 8.** Reflectance of the yellowish green sample. (For interpretation of the references to color in this figure legend, the reader is referred to the web version of this article.)

structure. Thickness of each layer are 21 nm, 39 nm, 16 nm, and 68 nm. The reflectance of the coating is lower than 10% in the wavelength range of 300–1170 nm and is lower than 5% in the visible spectral region, which results in a high solar absorbance (0.92), black appearance (as shown in the right down inset in Fig. 6), and a relatively low brightness (3.47%). The reflectance increases with increasing wavelength when $\lambda > 830$ nm and is higher than 50% as $\lambda > 1730$ nm, which contributes to a low thermal emittance (0.05).

The purple sample is also a Ti–AlN four layers structure and its reflectance is presented in Fig. 7. The reflectance of this coating decreases from 35% to 0% as the wavelength increases from 300 nm to 540 nm, and is lower than 6% when wavelength is between 540 nm and 1445 nm, which induces a high solar absorbance (0.94) and a very low brightness (0.65%). The purple color is the result from the maximum reflectance (10.5%) at 400 nm in visible region. A low thermal emittance (0.05) is caused by a reflectance larger than 50% as $\lambda > 2440$ nm.

As shown in Fig. 8, in order to obtain a green color, a AlN–Ti–AlN–Ti–AlN five layers structure was used in the yellowish green sample and the thickness of the first layer (AlN) is 269 nm, resulting in a reflectance with five peaks at wavelengths between 300 nm and 3439 nm. The reflectance of these peaks is 9.4% at 315 nm, 7.7% at 385 nm, 12.8% at 525 nm, 10.7% at 750 nm, and 55.7% at 1465 nm, inducing a relatively low solar absorbance (0.88) and a relatively high brightness (8.89%). Among these peaks, only the peak at 525 nm is in visible region, so the sample appears yellowish green. A relatively high thermal emittance (0.26) is because the reflectance is lower than 50% at wavelengths between 3439 nm and 6454 nm.

The red sample is also a five layers structure and its reflectance is presented in Fig. 9. Two high reflectance peaks of 27% at 655 nm and 64% at 1390 nm contribute to a low solar absorbance (82%) and a relatively high brightness (6.15%). The red color results from the peak at 655 nm. The reflectance has a minimum (1%) at 3364 nm, resulting in a relatively high thermal emittance (0.27).

Fig. 10 presents the reflectance of the yellowish orange sample. This coating is also a five layers structure and each layer thickness is lower than 70 nm. Reflectance is 0% at wavelength of 450 nm and 1460 nm, and there is a broad peak (15.4%) at 685 nm, which induces a high solar absorbance (0.92), a relatively high brightness (7.60%), and the yellowish orange appearance. This coating also has a low thermal emittance (0.06) since the reflectance is higher than 50% when the wavelength is longer than 2629 nm.

Fig. 11 shows the color coordinates of the five samples in the CIE tristimulus chromaticity diagram. The location of the black sample is very close to “neutral”, whereas the locations of other four samples are far from “neutral”, indicating that the solar absorbing coatings with different colors can be produced according to the optical design with a Ti–AlN multilayer structure.

In order to distinguish the performance of the five samples, their solar absorbance, thermal emittance, and brightness are tabulated in Table 2. The purple sample has the highest solar absorbance (0.94) and lowest brightness (0.65%). The yellowish green sample

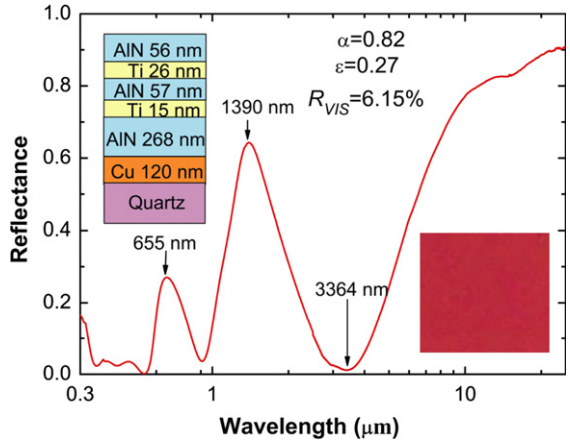


**Fig. 9.** Reflectance of the red sample. (For interpretation of the references to color in this figure legend, the reader is referred to the web version of this article.)

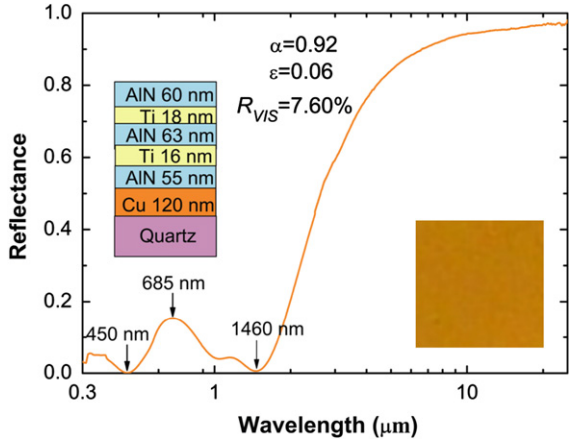


**Fig. 10.** Reflectance of the yellowish orange sample. (For interpretation of the references to color in this figure legend, the reader is referred to the web version of this article.)

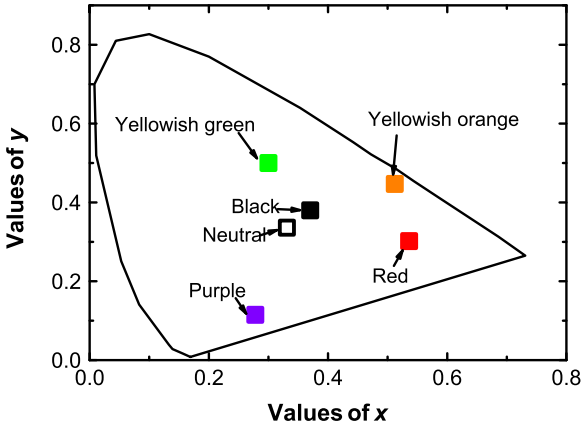


**Fig. 11.** Chromaticity diagram of the colored absorbing coatings.

has the highest brightness (8.89%), and the red sample has the lowest solar absorbance (0.82) and the highest thermal emittance (0.27). The yellowish orange sample has a good performance with respect to the other samples because its solar absorbance is 0.92, thermal emittance is 0.06, and brightness is 7.60%.

**Table 2**
Solar absorbance, thermal emittance, and brightness of the colored samples.

| Sample color | Black | Purple | Yellowish green | Red | Yellowish orange |
|---|---|---|---|---|---|
| $\alpha$ | 0.92 | 0.94 | 0.88 | 0.82 | 0.92 |
| $\varepsilon$ | 0.05 | 0.05 | 0.26 | 0.27 | 0.06 |
| $R_{VIS}$ (%) | 3.47 | 0.65 | 8.89 | 6.15 | 7.60 |

## 6. Conclusions

Ti and AlN single layer films with different thicknesses were deposited on quartz substrates by magnetron sputtering. The optical constants of the Ti and AlN films were retrieved from the transmittance or reflectance data by the optical dielectric models. It is found that both refractive indices and extinction coefficients of the Ti and AlN films increase with the increase of thickness. Based on the optical constants of the Ti and AlN films, five colored solar selective absorbing coatings with a Ti–AlN multilayer structure were designed by the optical multilayer software and prepared by magnetron sputtering. The color of the five samples is black, purple, yellowish green, red, and yellowish orange. The purple sample has the highest solar absorbance (0.94) and the lowest brightness (0.65%), and the yellowish green sample has the highest brightness (8.89%). The solar absorbance, thermal emittance, and brightness of the yellowish orange sample are 0.92, 0.06, and 7.60%, respectively. The results show that although these colored coatings present lower efficiency than the typical black type coatings, the difference in energy performance is at an acceptable level when we need esthetic compatibility of solar collectors with building architecture. Moreover, such colored coatings can be fabricated by a commercial production process.

## Acknowledgment

This work was financially supported by the Natural Science Foundation of China (No.: 11074041), and the Natural Science Foundation of Fujian Province of China (2012J01256).

## References

[1] N. Selvakumar, H.C. Barshilia, Review of physical vapor deposited (PVD) spectrally selective coatings for mid- and high-temperature solar thermal applications, Solar Energy Materials and Solar Cells 98 (2012) 1–23.
[2] Q.C. Zhang, Recent progress in high-temperature solar selective coatings, Solar Energy Materials and Solar Cells 62 (2000) 63–74.
[3] R.Z. Wang, X.Q. Zhai, Development of solar thermal technologies in China, Energy 35 (2010) 4407–4416.
[4] T.N. Anderson, M. Duke, J.K. Carson, The effect of colour on the thermal performance of building integrated solar collectors, Solar Energy Materials and Solar Cells 94 (2010) 350–354.
[5] Y. Tripanagnostopoulos, M. Souliotis, Th. Nousia, Solar collectors with colored absorbers, Solar Energy 68 (2000) 343–356.
[6] S. Kalogirou, Y. Tripanagnostopoulos, M. Souliotis, Performance of solar systems employing collectors with colored absorber, Energy and Buildings 37 (2005) 824–835.
[7] A. Schüler, C. Roecker, J.L. Scartezzini, J. Boudaden, I.R. Videnovic, R.S.C. Ho, P. Oelhafen, On the feasibility of colored glazed thermal solar collectors based on thin film interference filters, Solar Energy Materials and Solar Cells 84 (2004) 241–254.
[8] D. Zhu, S. Zhao, Chromaticity and optical properties of colored and black solar–thermal absorbing coatings, Solar Energy Materials and Solar Cells 94 (2010) 1630–1635.
[9] A. Schüler, C. Roecker, J. Boudaden, P. Oelhafen, J.L. Scartezzini, Potential of quarterwave interference stacks for colored thermal solar collectors, Solar Energy 79 (2005) 122–130.
[10] J. Boudaden, P. Oelhafen, A. Schüler, C. Roecker, J.L. Scartezzini, Multilayered $Al_2O_3/SiO_2$ and $TiO_2/SiO_2$ coatings for glazed colored solar thermal collectors, Solar Energy Materials and Solar Cells 89 (2005) 209–218.
[11] A. Schüler, J. Boudaden, P. Oelhafen, E.D. Chambrier, C. Roecker, J.L. Scartezzini, Thin film multilayer design types for colored glazed thermal solar collectors, Solar Energy Materials and Solar Cells 89 (2005) 219–231.

[12] J. Boudaden, R.S.C. Ho, P. Oelhafen, A. Schüler, C. Roecker, J.L. Scartezzini, Towards coloured glazed thermal solar collectors, Solar Energy Materials and Solar Cells 84 (2004) 225–239.
[13] D. Zhu, F. Mao, S. Zhao, The influence of oxygen in $TiAlO_xN_y$ on the optical properties of colored solar-absorbing coatings, Solar Energy Materials and Solar Cells 98 (2012) 179–184.
[14] X. Xiao, L. Miao, G. Xu, L. Lu, Z. Su, N. Wang, S. Tanemura, A facile process to prepare copper oxide thin films as solar selective absorbers, Applied Surface Science 257 (2011) 10729–10736.
[15] Z. Li, J. Zhao, L. Ren, Aqueous solution-chemical derived Ni–$Al_2O_3$ solar selective absorbing coatings, Solar Energy Materials and Solar Cells 105 (2012) 90–95.
[16] Y. Liu, C. Wang, Y. Xue, The spectral properties and thermal stability of NbTiON solar selective absorbing coating, Solar Energy Materials and Solar Cells 96 (2012) 131–136.
[17] N.P. Sergeant, O. Pincon, M. Agrawal, P. Peumans, Design of wide-angle solar-selective absorbers using aperiodic metal–dielectric stacks, Optics Express 17 (2009) 22800–22812.
[18] X.F. Li, Y.R. Chen, J. Miao, P. Zhou, Y.X. Zheng, L.Y. Chen, Y.P. Lee, High solar absorption of a multilayered thin film structure, Optics Express 15 (2007) 1907–1912.
[19] C.W. Chen, D.Y. Chen, C.Y. Hsu, Y.H. Chang, K.H. Hou, Spectrally selective Al/AlN/Al/AlN tandem solar absorber by inline reactive ac magnetron sputtering, Surface Engineering 27 (2011) 616–622.
[20] L. Gao, F. Lemarchand, M. Lequime, Comparison of different dispersion models for single layer optical thin film index determination, Thin Solid Films 520 (2011) 501–509.
[21] S. Esposito, A. Antonaia, M.L. Addonizio, S. Aprea, Fabrication and optimisation of highly efficient cermet-based spectrally selective coatings for high operating temperature, Thin Solid Films 517 (2009) 6000–6006.
[22] M. Du, L. Hao, J. Mi, F. Lv, X. Liu, L. Jiang, S. Wang, Optimization design of $Ti_{0.5}Al_{0.5}N/Ti_{0.25}Al_{0.75}N$/AlN coating used for solar selective applications, Solar Energy Materials and Solar Cells 95 (2011) 1193–1196.
[23] H. Savaloni, F. Farid-Shayegan, Film thickness dependence on the optical properties of sputtered and UHV deposited Ti thin films, Vacuum 85 (2010) 458–465.
[24] G. Yang, J. Sun, J. Zhou, Dielectric properties of aluminum silver alloy thin films in optical frequency range, Journal of Applied Physics 109 (2011) 123105 (6pp).
[25] S. Zhao, E. Wäckelgård, The optical properties of sputtered composite of Al–AlN, Solar Energy Materials and Solar Cells 90 (2006) 1861–1874.
[26] F. Lai, L. Lin, R. Gai, Y. Lin, Z. Huang, Determination of optical constants and thickness of $In_2O_3$:Sn films from transmittance data, Thin Solid Films 515 (2007) 7387–7392.
[27] M. Zheng, Y. Wu, L. Lin, W. Zheng, Y. Qu, F. Lai, Design and analysis of colored solar selective absorbing films with three-layer structure, Surface Review and Letters 19 (2012) 1250046 (7pp).
[28] M.A. Signore, A. Sytchkova, A. Rizzo, Sputtering deposition and characterization of tandem absorbers for photo-thermal systems operating at mid temperature, Optical Materials 34 (2011) 292–297.
[29] F. Lai, Y. Wang, M. Li, H. Wang, Y. Song, Y. Jiang, Determination of optical constants and inhomogeneity of optical films by two-step film envelope method, Thin Solid Films 515 (2007) 4763–4767.
[30] F. Lai, L. Lin, Z. Huang, R. Gai, Y. Qu, Effect of thickness on the structure, morphology and optical properties of sputter deposited $Nb_2O_5$ films, Applied Surface Science 253 (2006) 1801–1805.
[31] Software Spectra, Inc. Version: TFCalc 3.5, ⟨http://www.sspectra.com/⟩.